A Comparison of Recurrent and Convolutional Deep Learning Architectures for EEG Seizure Forecasting

Sina Shafiezadeh[1][a], Marco Pozza[2][b] and Alberto Testolin[1,2][c]

[1]*Department of General Psychology, University of Padova, Padova, Italy*

[2]*Department of Mathematics, University of Padova, Padova, Italy*

fi

Keywords: Seizure Prediction, Epilepsy, Artificial Intelligence, Convolutional Neural Networks, Long Short-Term Memory Networks, Electroencephalography, Signal Processing, Scalogram Images.

Abstract: Many research efforts are being spent to discover predictive markers of seizures, which would allow to build forecasting systems that could mitigate the risk of injuries and clinical complications in epileptic patients. Although electroencephalography (EEG) is the most widely used tool to monitor abnormal brain electrical activity, no commercial devices can reliably anticipate seizures from EEG signal analysis at present. Recent advances in Artificial Intelligence, particularly deep learning algorithms, show promise in enhancing EEG classifier forecasting accuracy by automatically extracting relevant spatio-temporal features from EEG recordings. In this study, we systematically compare the predictive accuracy of two leading deep learning architectures: recurrent models based on Long Short-Term Memory networks (LSTMs) and Convolutional Neural Networks (CNNs). To this aim, we consider a data set of long-term, continuous multi-channel EEG recordings collected from 29 epileptic patients using a standard set of 20 channels. Our results demonstrate the superior performance of deep learning algorithms, which can achieve up to 99% accuracy, sensitivity, and specificity compared to more traditional machine learning approaches, which settle around 75% in all evaluation metrics. Our results also show that giving as input the recordings from all electrodes allows to exploit useful channel correlations to learn more robust predictive features, compared to convolutional models that treat each channel independently. We conclude that deep learning architectures hold promise for enhancing the diagnosis and prediction of epileptic seizures, offering potential benefits to those affected by such invalidating neurological conditions.

1 INTRODUCTION

Epilepsy, a chronic neurological disorder that affects approximately 50 million people worldwide of all ages, is characterized by recurring seizures, often accompanied by loss of consciousness and control of bladder or bowel function (World Health Organization, 2023). EEG is considered a promising, non-invasive clinical diagnostic method that could be used to continuously monitor brain electrical activity, potentially allowing for automatic detection or even forecasting epileptic seizures in advance (Van Mierlo et al., 2020). A reliable monitoring device would allow patients to avoid dangerous situations or even plan the administration of preventive treatments, such as electrical stimulation or targeted drug delivery, thus

[a] https://orcid.org/0000-0002-5462-4893
[b] https://orcid.org/0009-0004-5798-0297
[c] https://orcid.org/0000-0001-7062-4861

significantly improving their quality of life.

In recent years, the growing effectiveness of deep learning methods in clinical diagnosis and disease prediction (Liu et al., 2020; Calesella et al., 2021) has reignited enthusiasm for harnessing machine learning algorithms in the complex task of seizure forecasting (Abbasi and Goldenholz, 2019). It should be noted that seizure forecasting aims to anticipate an upcoming seizure before it clinically manifests, making this task much more challenging compared to seizure detection, a simpler classification problem that requires discriminating between normal brain activity and seizure states. A common strategy to implement predictive models involves extracting diverse descriptive characteristics from EEG recordings, which are then used to train machine learning algorithms to recognize time intervals close to an imminent seizure (Assi et al., 2017). However, the most recent approaches exploit deep learning techniques, which can

achieve higher accuracy by extracting more sophisticated, non-linear features directly from the raw signals (Usman et al., 2020).

Several deep learning architectures have been proposed to process EEG signals efficiently. Long Short-Term Memory (LSTM) networks (Hochreiter and Schmidhuber, 1997) are particularly effective in learning temporal features from time series and have thus been widely applied to the automatic analysis of EEG recordings, with promising results also in some seizure prediction tasks (Tsiouris et al., 2018; Varnosfaderani et al., 2021). CNNs are instead effective in discovering spatial features from images, but can also be used to analyze windowed signals extracted from time series (LeCun et al., 1995) and have thus been successfully applied to EEG seizure prediction (San-Segundo et al., 2019; Hussein et al., 2021). Moreover, some authors have proposed to enhance the classic 2D convolutional architecture by introducing 3D convolutions, enabling the extraction of features from both spatial and temporal dimensions and the discovery of correlations between feature maps and contiguous frames in the previous layer (Ji et al., 2012). In EEG signal analysis, this allows to consider inter-channel correlations, which can be particularly useful when classifying preictal and interictal seizure states (Wang et al., 2021; Ozcan and Erturk, 2019).

In this study, we compare the performance of LSTMs, 2D CNNs, and 3D CNNs in the challenging task of seizure forecasting. For the LSTM, we directly fed the model the raw signals recorded from all EEG channels, which should allow the network to exploit both temporal and inter-channel features to carry out the prediction task. For the 2D CNN, we gave images as input to the model representing the scalogram of windowed EEG signals recorded from each channel independently. For the 3D CNN, the input is instead constituted by the image scalogram of all channels, which similarly to the LSTM case should allow the network to exploit inter-channel dependencies besides spatio-temporal features extracted from each individual scalogram.

We hypothesize that deep learning models would achieve higher predictive performance compared to standard machine learning algorithms, such as those based on eXtreme Gradient Boosting (XGBoost) (Shafiezadeh et al., 2023), and that neural architectures that exploit inter-channel correlations such as the LSTM and the 3D CNN would result in better forecast accuracy.

2 METHODS

2.1 EEG Data Set

We used a data set of long-term, continuous multi-channel EEG recordings collected by the Epilepsy and Clinical Neurophysiology Unit at the Eugenio Medea IRCCS Hospital in Conegliano, Italy. EEG data were recorded from 29 epileptic patients (15 males and 14 females) at a sampling rate of 256 Hz. We selected 20 common channels based on the international standard 10-20 EEG scalp electrode positioning system (see Fig. 1).

Each seizure event was characterized by four possible states: preictal, ictal, postictal, and interictal. These states correspond to the periods before the onset of a seizure, the onset and conclusion of a seizure, the period following a seizure, and normal brain activity, respectively. In our data, the onset and termination of ictal states were manually identified using video recorded data from video-EEG monitoring by two expert clinicians. The seizure prediction task was framed as a binary classification problem of diagnosing preictal (30 minutes preceding a seizure) vs. interictal (30 to 120 minutes preceding a seizure) states. To guarantee the use of proper interictal time periods, we excluded seizures occurring in recordings shorter than 3 hours, resulting in a total of 93 seizures retained for subsequent analysis. However, all seizures were randomized together for cross-validation and dividing the data into train and test data points.
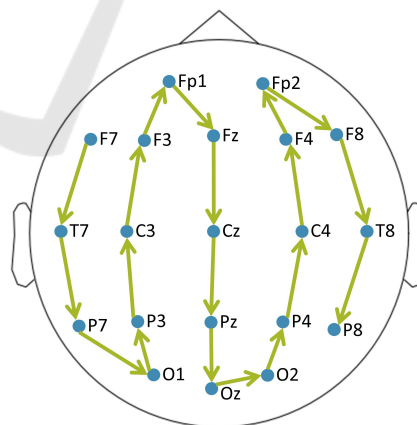

Figure 1: The 20 common channels were used in this study. The channels ordering process initiates from the left temporal lobe (starting from F7) and extends to the right temporal lobe (ending to P8). This deliberate sequence was designed to formulate 3D inputs as a stack of 2D segments incorporating inter-channel correlations.

2.2 EEG Signal Pre-Processing

Several filtering procedures were applied to enhance signal quality. Specifically, a 125 Hz low-pass filter and a 1 Hz high-pass filter were applied to retain high-frequency signals relevant to abnormal brain activities before seizures, while simultaneously removing DC offset and baseline fluctuations (Allen et al., 1992; Arroyo and Uematsu, 1992). Moreover, to mitigate power line interference, two notch filters operating at 50 Hz and 100 Hz were incorporated in the pre-processing pipeline (Niknazar et al., 2015; Thangavel et al., 2021). EEG signals were finally downsampled to 128 Hz, and the time series were normalized by subtracting the average EEG reference computed on each patient's training data. All filtering operations were performed using the MNE package within the Python 3.8.5 version.

2.3 Scalogram Images

The input matrices for CNN models were created by transforming the EEG time series into scalogram images, as proposed in recent studies (Yildiz et al., 2021; Varlı and Yılmaz, 2023). To this aim, the Continuous Wavelet Transform (CWT) was used to compute multiple expansions and the wavelet's time offset, yielding a variety of frequency values for analyzing continuous-time signals that can be used to characterize energy density at a local time-frequency within the transformation (Peng et al., 2002). A more precise and flexible time–frequency resolution can be obtained by considering the absolute value of the CWT when producing scalogram images (Bostanov, 2004), which is particularly effective since it effectively captures high- and low-frequency information also in non-stationary signals like EEG (Falamarzi et al., 2014).

More precisely, a function known as the main wavelet performs the window's role within the wavelet transform; during the conversion process, this main wavelet function is scaled and shifted, enabling extensive time interval windowing for low frequencies and compressed time interval windowing for high frequencies (Türk and Özerdem, 2019). The Morlet wavelet was employed for the continuous wavelet transformations (Kareem and Kijewski, 2002). CWT can be represented mathematically in continuous time as in Equation (1), where W(s, τ), x(t), (t), s, and τ represent the wavelet coefficients, the time signal, the basic wavelet function conjugate, the scale, and the position parameter, respectively:

$$W_x(s,\tau) = \frac{1}{\sqrt{s}} \int_{-\infty}^{+\infty} x(t)\psi^*\left(\frac{t-\tau}{s}\right)dt \qquad (1)$$

In our study, scalogram images were created using sliding windows of 30 seconds with 50% overlap, resulting in greater accuracy compared to shorter windows of 10 or 20 seconds. To improve computational efficiency during model training, the resulting time-frequency scalogram images were resized to 96 × 96 pixels using cubic interpolation, following the methodology adopted by (Ozdemir et al., 2021) and (Türk and Özerdem, 2019). Samples of resized scalograms depicting distinct preictal and interictal states are shown in Fig. 2.

2.4 Deep Learning Architectures

All models were implemented using the PyTorch framework (version 1.13.0). Training and testing phases were carried out using a virtual machine equipped with an Nvidia V100 GPU allocated in the Google Cloud Platform.

2.4.1 Hyperparameters Tuning

Model hyperparameters were iteratively refined using a hierarchical strategy to attain the optimal configuration using a reasonable amount of computing time. For the LSTM model we tuned the hyperparameters using the Optuna framework (Akiba et al., 2019); the search space included the number of hidden layers (1, 2, 3), the size of hidden layers (32, 64, 128, 256), learning rate (1e-5 to 0.1), batch size (16, 32, 64, 128, 256), and the dropout rates (0.1 to 0.9). The CNNs hyperparameters were tuned in a specific order, starting from the number of hidden layers (2, 3, 4), the number of kernels (16, 32, 64), the kernel size (2, 3, 5), the learning rate (0.01, 0.001, 0.0001), the number of dropout layers (1, 2, 3), the dropout rate (0.1, 0.2, 0.5), batch size (16, 32, 64) and the use of pooling layers to reduce the size of feature maps progressively. The hyperparameters yielding the best performance at each step were selected before progressing to the next optimization step.

2.4.2 LSTM

The LSTM network received an input time series of 5-second raw signals with a 3-second overlap, resulting in an input size of 20 channels × 640 time points. The final LSTM architecture was made up of two hidden layers, with 32 units each. Two drop-out layers with a drop-out rate of 0.1 and 0.3 were included between the two LSTM layers and before the fully connected layer, respectively. The final LSTM architecture is represented in Fig. 3.
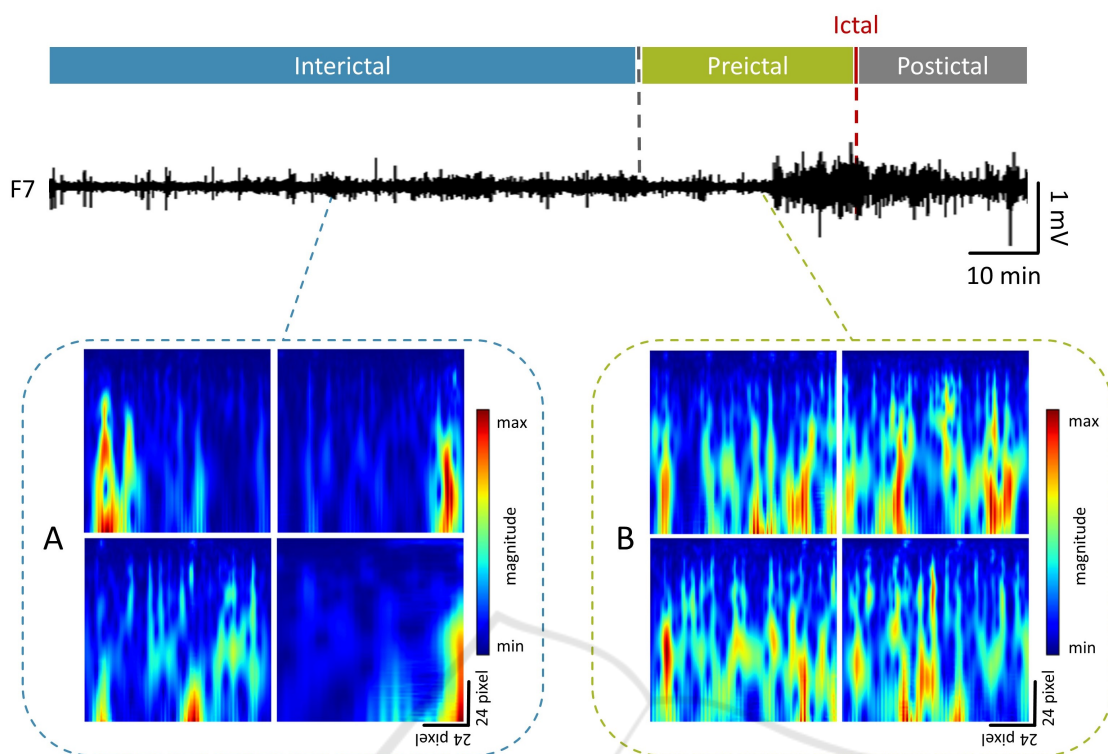
Figure 2: Example of a 145 min EEG signal trace recorded from channel F7 during a seizure event, segmented to identify interictal vs. preictal states. Panel A shows four different sample images from the interictal state, while panel B shows four different sample images from the preictal state.

2.4.3 2D CNN

For the 2D convolutional network, scalogram images originating from each channel were treated independently. Consequently, the input dimension for the 2D model was 96×96. The final architecture comprised three convolutional layers, with 16, 32, and 64 kernels, activated by Rectified Linear Unit (ReLU) functions and complemented with batch normalization layers. The optimal kernel size was 3×3 for all layers, and a stride of 3 and padding of one pixel was applied. To mitigate the risk of overfitting, two dropout layers with a dropout rate of 0.1 were placed after the third convolutional layer and the flatting layer. The flattened layer was further processed by an additional ReLU-activated dense layer comprising 128 units, and this layer was finally decoded by an output layer that used a sigmoid activation function to produce the model's prediction.

2.4.4 3D CNN

To create the 3D input, a specific order of channels from the left to the right temporal lobe was adopted: F7, T7, P7, O1, P3, C3, F3, Fp1, Fz, Cz, Pz, Oz, O2, P4, C4, F4, Fp2, F8, T8, and P8 (see Fig. 1). The

corresponding scalogram images were given as input to the 3D model, resulting in a $20 \times 96 \times 96$ input shape. To allow for a fair comparison, the existing 2D CNN optimal architecture was subject to adaptation solely in terms of kernel dimensions, transitioning from 2D to 3D. The final 3D architecture is represented in Fig. 4.

2.5 Model Evaluation

All models were trained for 100 epochs, and the training accuracy was recorded after each epoch in order to track learning progress over time. Furthermore, randomized cross-validation was carried out in each fold by dividing the 93 seizures into 80% train and 20% test sets. However, during the five-fold cross-validation implementation, the average accuracy of testing data points after each fold was considered to select the best model and compare three models. Models' performances were measured using 5-fold cross-validation in terms of accuracy (ACC), sensitivity (SEN), and specificity (SPE), which were computed from true positives (TP), false positives (FP), true negatives (TN), and false negatives (FN) as follows:
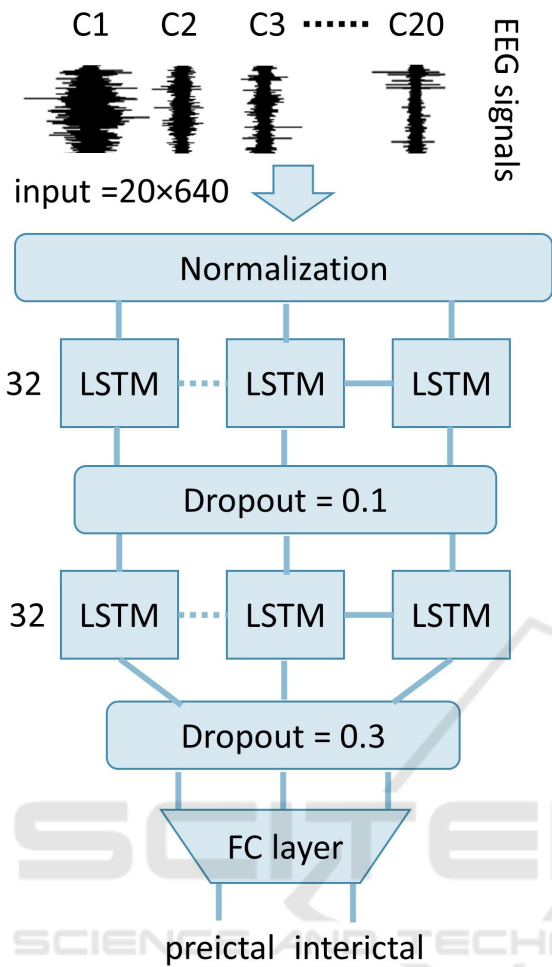
Figure 3: Representation of the final LSTM model architecture. The model comprises two LSTM layers with 32 units each and two drop-out layers with 0.1 and 0.3 rates, respectively.

$$Accuracy = ((tp + tn)/(tp + tn + fn + fp)) \quad (2)$$

$$Sensitivity = (tp/(tp + fn)) \quad (3)$$

$$Specificity = (tn/(tn + fp)) \quad (4)$$

In order to evaluate the performance gain of deep learning models compared to traditional machine learning classifiers, the best-performing architectures were further benchmarked against an XGBoost classifier trained on a set of 53 EEG features (for details, see (Shafiezadeh et al., 2023)).
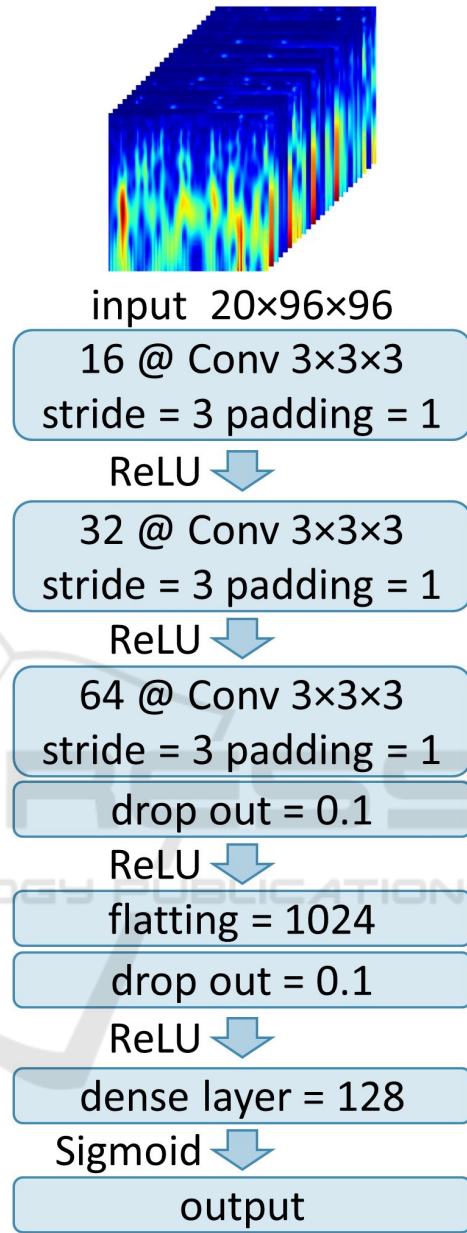

Figure 4: Representation of the final 3D CNN model architecture. The model comprises three convolutional layers and two drop-out layers. The 2D CNN architecture is identical, with a kernel dimension of 3 × 3.

3 RESULTS

As shown in Figure 5, the LSTM model converged to higher accuracy in a smaller number of training epochs. The final performance of the 2D model was significantly lower than the LSTM and 3D models, suggesting that inter-channel correlations constitute
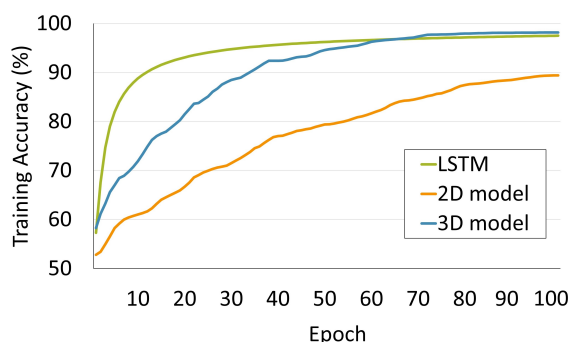
Figure 5: Improvement of training accuracy during the fitting of the three deep learning models (3D, LSTM, and 2D).
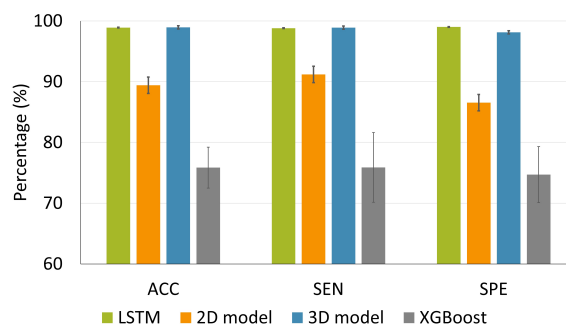

Figure 6: Comparison of the average performance metrics of the testing set for classifying interictal and preictal phases with the LSTM, 2D, 3D, and XGBoost models. Error bars represent the standard deviation of each performance metric after the implementation of five-fold cross-validation.

an important source of information that can be leveraged for the seizure prediction task.

In the testing phase, the LSTM model achieved the highest specificity at 99.01%, while the 3D model exhibited the highest accuracy and sensitivity, with values of 98.95% and 98.91%, respectively. ACC, SEN, and SPE average values of each model in the testing set, as well as standard deviations of each testing set's performance metric after implementation of five-fold, are presented in Table 1. This table also illustrates the results of statistical comparisons (one-way ANOVA) between the three models after tuning and their best results. The findings show significant differences between all performance metrics, and post-hoc Tukey tests confirmed that the 2D architecture performed worse than the LSTM and the 3D architectures (see Table 2).

The LSTM model demonstrated significant improvements in performance metrics compared to the 2D model, with differences of 9.49%, 7.62%, and 12.46% in ACC, SEN, and SPE, respectively. Also, the 3D model achieved substantial improvements compared to the 2D model, respectively of 9.53%, 7.72%, and 11.57%. Although slight variations exist in the performance metrics between the LSTM and the 3D model, such differences were not statistically significant. A graphical representation of all performance metrics is given in Figure 6.

3.1 Comparison with XGBoost

Having identified the LSTM and 3D models as the top-performing models according to all performance metrics, we then proceeded with a comparison against a standard machine learning model, specifically XGBoost, trained on a set of 53 ad hoc features extracted from the EEG signal (for details, see (Shafiezadeh et al., 2023)). The performance metrics of XGBoost are shown in the gray column of Figure 6.

After applying cross-validation on the fea-

ture data set, the XGBoost model achieved ACC (75.86%±3.37), SEN (75.90%±5.74), and SPE (74.72%±4.61). The LSTM model significantly outperformed XGBoost across all evaluation metrics: 23.05% in ACC, 22.91% in SEN, and 24.29% in SPE (all p-values <0.01). The same results were found for the 3D model, which significantly outperformed XGBoost with increases of 23.09% in ACC, 23.01% in SEN, and 23.40% in SPE (all p-values <0.01). It is also worth noting that deep learning models are associated with substantially reducing the standard error associated with each evaluation metric, suggesting a more stable classification performance.

4 DISCUSSION

In this study, we leveraged raw signals and scalogram images derived from multichannel EEG recordings of epileptic patients to conduct a comparative analysis between the LSTM, 2D, and 3D models in seizure forecasting. Our investigation revealed that incorporating inter-channel correlations by feeding all channels to the LSTM model and the 3D CNN model yielded a significant (almost 10%) improvement in accuracy, increasing the classifier precision in distinguishing between interictal and preictal states.

A direct benchmarking against a more traditional XGBoost machine learning classifier further confirmed that deep learning architectures allow to achieve substantial performance gains across all evaluation metrics. At the same time, it should be noted that our results are not directly comparable with other recently published findings, since our analyses were carried out using a novel clinical dataset recently collected in a local hospital. However, as a qualitative comparison, we might argue that our findings

Table 1: Average accuracy (ACC), sensitivity (SEN), and specificity (SPE) of the testing set obtained by different architectures. All performance metrics are illustrated by mean(%)±standard deviation after the implementation of five-fold cross-validation. The last two columns report the results from the ANOVA.

Metrics	LSTM	2D	3D	F-value	p-value
ACC	98.91±0.34	89.42±1.13	98.95±0.39	234.96	<0.01
SEN	98.81±0.56	91.19±3.79	98.91±0.26	15.97	<0.01
SPE	99.01±0.75	86.55±2.23	98.12±0.73	95.30	<0.01

Table 2: Results of the Tukey post-hoc test to compare performance metrics of the LSTM, 2D, and 3D models. Each row in the table corresponds to the p-value calculated for the comparison between two target models in terms of accuracy (ACC), sensitivity (SEN), and specificity (SPE) of the testing set.

Models	ACC	SEN	SPE
LSTM - 2D	<0.01	<0.05	<0.01
LSTM - 3D	0.996	0.998	0.660
3D - 2D	<0.01	<0.01	<0.01

are well-aligned, if not superior, with the accuracy and sensitivity levels reported in the recent literature: for example, LSTMs achieved an accuracy of 85.1% and a sensitivity of 86.8% in a similar seizure prediction task (Varnosfaderani et al., 2021), and 3D CNNs have been recently shown able to reach an accuracy of 80.50% (Wang et al., 2021) and sensitivity of 85.7% (Ozcan and Erturk, 2019) in seizure prediction.

5 CONCLUSIONS

While several studies have recently demonstrated that deep learning models can achieve high accuracy in seizure prediction tasks by analyzing EEG recordings from individual channels, our study suggests that feeding multiple channels simultaneously, as it happens in the LSTM and 3D CNN architectures, allows to exploit inter-channel correlations to improve forecasting performance. Furthermore, our results show that deep learning methods significantly outperform traditional machine learning approaches, supporting the recent trend of applying neural network models to the automated analysis of biological signals.

For future work, it would be interesting to investigate channel selection techniques (Jana and Mukherjee, 2021) to further establish whether some channels are more important than others in the seizure prediction task. Especially for focal epilepsy, this would likely depend on the localization of the seizure source (e.g., temporal vs. occipital). It would thus be crucial to collect EEG recordings from a larger cohort of patients in order to make it possible to train source-specific models and/or exploit a more heterogeneous training set to extract generalizable features that can

be used across different patients' profiles. A related research direction would be to move from randomized cross-validation setups to more robust evaluation schemes, such as those based on leave-one-patient-out cross-validation (Shafiezadeh et al., 2023). However, this would also require to significantly scale-up the available training datasets, which should allow to discover more robust predictive features.

Last but not least, it would be important to design and implement interpretability methods that can be used to better understand the output produced by deep learning models. Indeed, in medical settings it is of paramount importance to deploy explainable AI methods to improve the reliability of automatic decision systems (Gunning et al., 2019).

REFERENCES

Abbasi, B. and Goldenholz, D. M. (2019). Machine learning applications in epilepsy. *Epilepsia*, 60(10):2037–2047.

Akiba, T., Sano, S., Yanase, T., Ohta, T., and Koyama, M. (2019). Optuna: A next-generation hyperparameter optimization framework. In *Proceedings of the 25rd ACM SIGKDD International Conference on Knowledge Discovery and Data Mining*.

Allen, P., Fish, D., and Smith, S. (1992). Very high-frequency rhythmic activity during EEG suppression in frontal lobe epilepsy. *Electroencephalography and clinical neurophysiology*, 82(2):155–159.

Arroyo, S. and Uematsu, S. (1992). High-frequency EEG activity at the start of seizures. *Journal of Clinical Neurophysiology*, 9(3):441–448.

Assi, E. B., Nguyen, D. K., Rihana, S., and Sawan, M. (2017). Towards accurate prediction of epileptic seizures: A review. *Biomedical Signal Processing and Control*, 34:144–157.

Bostanov, V. (2004). Bci competition 2003-data sets ib and iib: feature extraction from event-related brain potentials with the continuous wavelet transform and the t-value scalogram. *IEEE Transactions on Biomedical engineering*, 51(6):1057–1061.

Calesella, F., Testolin, A., De Filippo De Grazia, M., and Zorzi, M. (2021). A comparison of feature extraction methods for prediction of neuropsychological scores from functional connectivity data of stroke patients. *Brain Informatics*, 8(1):1–13.

Falamarzi, Y., Palizdan, N., Huang, Y. F., and Lee, T. S. (2014). Estimating evapotranspiration from temperature and wind speed data using artificial and wavelet neural networks (wnns). *Agricultural Water Management*, 140:26–36.

Gunning, D., Stefik, M., Choi, J., Miller, T., Stumpf, S., and Yang, G.-Z. (2019). Xai—explainable artificial intelligence. *Science robotics*, 4(37):eaay7120.

Hochreiter, S. and Schmidhuber, J. (1997). Long short-term memory. *Neural computation*, 9(8):1735–1780.

Hussein, R., Lee, S., Ward, R., and McKeown, M. J. (2021). Semi-dilated convolutional neural networks for epileptic seizure prediction. *Neural Networks*, 139:212–222.

Jana, R. and Mukherjee, I. (2021). Deep learning based efficient epileptic seizure prediction with EEG channel optimization. *Biomedical Signal Processing and Control*, 68:102767.

Ji, S., Xu, W., Yang, M., and Yu, K. (2012). 3d convolutional neural networks for human action recognition. *IEEE transactions on pattern analysis and machine intelligence*, 35(1):221–231.

Kareem, A. and Kijewski, T. (2002). Time-frequency analysis of wind effects on structures. *Journal of Wind Engineering and Industrial Aerodynamics*, 90(12-15):1435–1452.

LeCun, Y., Bengio, Y., et al. (1995). Convolutional networks for images, speech, and time series. *The handbook of brain theory and neural networks*, 3361(10):1995.

Liu, Y., Jain, A., Eng, C., Way, D. H., Lee, K., Bui, P., Kanada, K., de Oliveira Marinho, G., Gallegos, J., Gabriele, S., et al. (2020). A deep learning system for differential diagnosis of skin diseases. *Nature medicine*, 26(6):900–908.

Niknazar, H., Maghooli, K., and Nasrabadi, A. M. (2015). Epileptic seizure prediction using statistical behavior of local extrema and fuzzy logic system. *international journal of computer applications*, 113(2).

Ozcan, A. R. and Erturk, S. (2019). Seizure prediction in scalp EEG using 3d convolutional neural networks with an image-based approach. *IEEE Transactions on Neural Systems and Rehabilitation Engineering*, 27(11):2284–2293.

Ozdemir, M. A., Cura, O. K., and Akan, A. (2021). Epileptic EEG classification by using time-frequency images for deep learning. *International journal of neural systems*, 31(08):2150026.

Peng, Z., Chu, F., and He, Y. (2002). Vibration signal analysis and feature extraction based on reassigned wavelet scalogram. *Journal of Sound and Vibration*, 253(5):1087–1100.

San-Segundo, R., Gil-Martin, M., D'Haro-Enríquez, L. F., and Pardo, J. M. (2019). Classification of epileptic EEG recordings using signal transforms and convolutional neural networks. *Computers in biology and medicine*, 109:148–158.

Shafiezadeh, S., Duma, G. M., Mento, G., Danieli, A., Antoniazzi, L., Del Popolo Cristaldi, F., Bonanni, P., and Testolin, A. (2023). Methodological issues in evaluating machine learning models for EEG seizure prediction: Good cross-validation accuracy does not guarantee generalization to new patients. *Applied Sciences*, 13(7):4262.

Thangavel, P., Thomas, J., Peh, W. Y., Jing, J., Yuvaraj, R., Cash, S. S., Chaudhari, R., Karia, S., Rathakrishnan, R., Saini, V., et al. (2021). Time–frequency decomposition of scalp electroencephalograms improves deep learning-based epilepsy diagnosis. *International journal of neural systems*, 31(08):2150032.

Tsiouris, K. M., Pezoulas, V. C., Zervakis, M., Konitsiotis, S., Koutsouris, D. D., and Fotiadis, D. I. (2018). A long short-term memory deep learning network for the prediction of epileptic seizures using EEG signals. *Computers in biology and medicine*, 99:24–37.

Türk, Ö. and Özerdem, M. S. (2019). Epilepsy detection by using scalogram based convolutional neural network from EEG signals. *Brain sciences*, 9(5):115.

Usman, S. M., Khalid, S., and Aslam, M. H. (2020). Epileptic seizures prediction using deep learning techniques. *Ieee Access*, 8:39998–40007.

Van Mierlo, P., Vorderwülbecke, B. J., Staljanssens, W., Seeck, M., and Vulliémoz, S. (2020). Ictal EEG source localization in focal epilepsy: Review and future perspectives. *Clinical Neurophysiology*, 131(11):2600–2616.

Varlı, M. and Yılmaz, H. (2023). Multiple classification of EEG signals and epileptic seizure diagnosis with combined deep learning. *Journal of Computational Science*, 67:101943.

Varnosfaderani, S. M., Rahman, R., Sarhan, N. J., Kuhlmann, L., Asano, E., Luat, A., and Alhawari, M. (2021). A two-layer lstm deep learning model for epileptic seizure prediction. In *2021 IEEE 3rd International Conference on Artificial Intelligence Circuits and Systems (AICAS)*, pages 1–4. IEEE.

Wang, Z., Yang, J., and Sawan, M. (2021). A novel multiscale dilated 3d cnn for epileptic seizure prediction. pages 1–4.

World Health Organization (2023). Epilepsy, https://www.who.int/en/news-room/fact-sheets/detail/epilepsy.

Yildiz, A., Zan, H., and Said, S. (2021). Classification and analysis of epileptic EEG recordings using convolutional neural network and class activation mapping. *Biomedical signal processing and control*, 68:102720.